

Electronic supplementary information (ESI) available

Nonlinear Rashba Spin Splitting in Transition Metal Dichalcogenide Monolayers

Cai Cheng^{a,b}, Jia-Tao Sun^{*,a}, Xiang-Rong Chen^{*,b}, Hui-Xia Fu^a, Sheng Meng^{*,a,c}

^aBeijing National Laboratory for Condensed Matter Physics and Institute of Physics, Chinese Academy of Sciences, Beijing 100190, China

^bCollege of Physical Science and Technology, Sichuan University, Chengdu 610064, China

^cSchool of Physical Sciences, University of Chinese Academy of Sciences, Beijing 100190, China

1. Atomic and electronic structures of monolayer TMDs

The atomic structures of the monolayers MXY (M = Mo, W; X, Y = S, Se) is shown in Figure 1a. When d_{M-X} is equal to d_{M-Y} , MXY becomes non-polar systems, such as MoS₂, MoSe₂ and WS₂. When d_{M-X} is not equal to d_{M-Y} , MXY denotes for MoSSe with an out-of-plane dipole moment (Figure S2b). The lattice parameters of MoSSe are $a_0=3.25$ Å, $\Delta_d=3.23$ Å, $d_{M-X}=2.42$ Å, $d_{M-Y}=2.53$ Å, respectively. The lattice constants are well consistent with the results of Zhu *et. al.*,¹ Cheng *et. al.*² and Zhuang *et. al.*³ More details structural information is presented in Table S1. The phonon dispersion of MXY is plotted in Figure S1 No imaginary frequency indicates that the MXY can be dynamically stable under strong electric field.

Table S1. Structural and electronic parameters of MXY. Lattice constant a_0 (Å), layer thickness Δ_d (Å), the energy difference Δ_{K-K} , $\Delta_{K-\Gamma}$ (denoted in Figure 2 in the main text) without or with spin-orbit coupling (SOC) and spin splitting Δ_{K-SOC} (meV) of the top valence band at K-point.

MXY	(SOC)	a_0 (Å)	Δ_d (Å)	Δ_{K-SOC} (meV)	Δ_{K-K} (eV)	$\Delta_{K-\Gamma}$ (meV)
MoS ₂	w/o-soc	3.18	3.13	-	1.68	29.7
	w/-soc			149.0	1.60	100.8
MoSe ₂	w/o-soc	3.32	3.34	-	1.43	261.7
	w/-soc			185.7	1.33	341.6
WS ₂	w/o-soc	3.182	3.14	-	1.81	62.4
	w/-soc			429.8	1.55	257.2
MoSSe	w/o-soc	3.25	3.23	-	1.56	13.9
	w/-soc			169.5	1.46	88.8

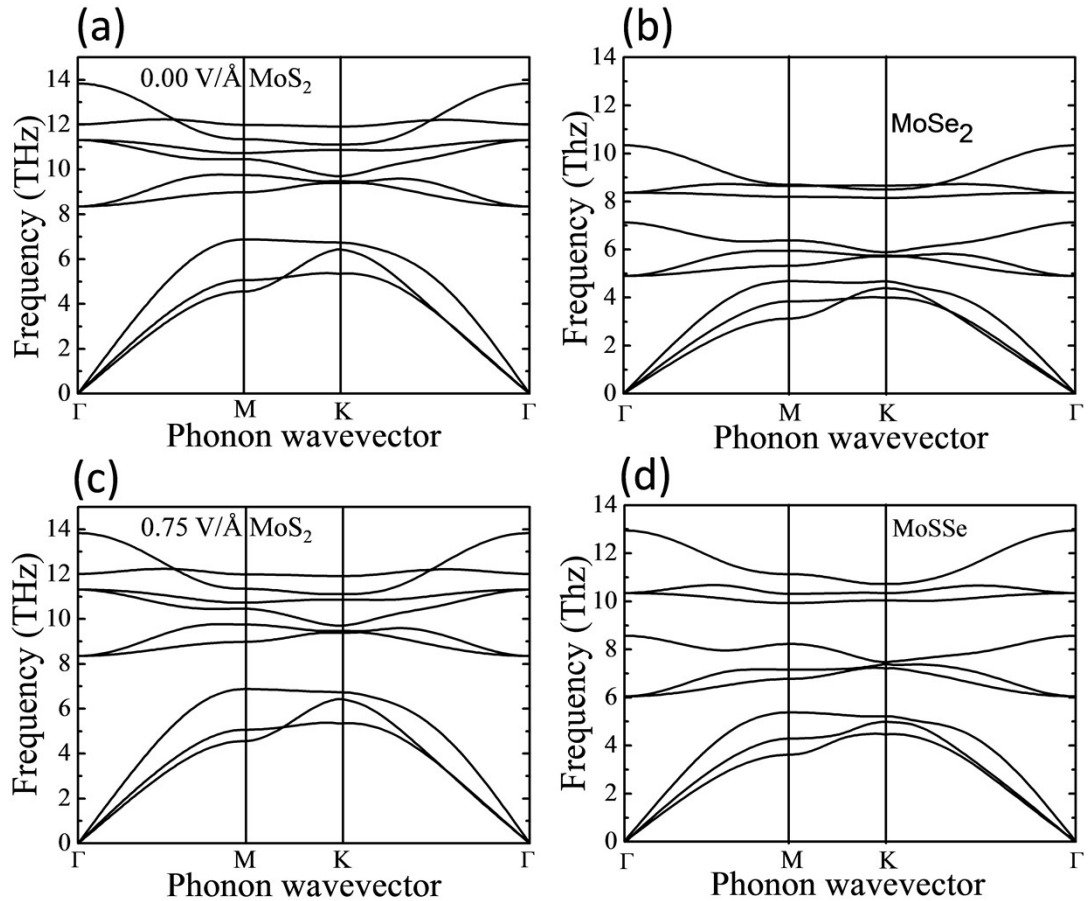


Figure S1 (a), (c) Phonon dispersion of MoS₂ without and with the external electric field. For comparison, the MoSSe and MoSe₂ are also shown (b), (d). The absence of imaginary frequency indicates the stability of monolayer TMDs.

Extensive experimental and theoretical studies have been reported on the electronic

structure of few-layer TMDs. The interlayer interaction leads to remarkable modifications of the electronic and optical properties of MX_2 . A transition from indirect (bulk or few-layer) to direct band gap (monolayer) is found.⁴⁻⁶ Moreover, the valence band maximum (VBM) and conduction band minimum (CBM) are located at the K-point for the monolayer, while the bulk phase has the VBM at the K point and the CBM along the Γ -K line. According to Table S1, the monolayers MoS_2 , MoSe_2 , WS_2 as well as MoSSe are direct band gap semiconductor independent on including the spin-orbital coupling (SOC). From the Table S1, the band gaps with the SOC are smaller than these without SOC case. The spin splitting of the uppermost valence band at K point $\Delta_{\text{K-SOC}}$ (meV) are 149.0, 169.5, 185.7, and 429.8 in MoS_2 , MoSSe , MoSe_2 and WS_2 respectively.

2. The planar averaged electrostatic potential and dipole moment

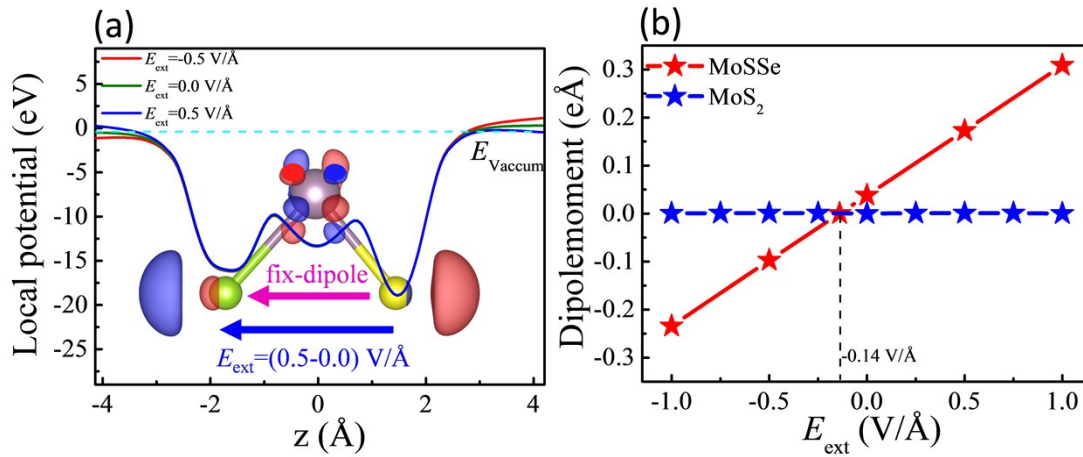


Figure S2 (a) The planar averaged local potential of MoSSe with the external electric field of -0.5 V/\AA (red), 0.0 V/\AA (olive), and 0.5 V/\AA (blue). The potential data are shifted with respect to the vacuum level (zero energy). The intrinsic dipole from S to Se (it is due to the lower potential to higher potential). The inset is the charge density difference between $E_{\text{ext}} = 0.5 \text{ V/\AA}$ and $E_{\text{ext}} = 0 \text{ V/\AA}$. Red (blue) color represents the electron accumulation (depletion) region. The isosurface value is set to 0.0038 e/\AA^3 . (b) The dipole moment vary with the extra electric field E_{ext} .

The Rashba effect has been reported in the polar-system MoSSe .² No Rashba splitting has been reported in non-polar system MX_2 due to the mirror symmetry $(x, y, z) \rightarrow (x, y, -z)$

vanishing the potential gradients. The mirror symmetry can be broken by the perpendicular extra electric field E_{ext} . However the emergence of Rashba effect of MX_2 and MoSSe originates from the potential gradient around the sulfur atoms under the electric field as described in the main text. In order to distinguish the intrinsic difference of the polar MoSSe and non-polar MoS_2 , Figure S2 shows the variation of dipole moment with the extra electric field E_{ext} . It can be clearly seen that the dipole moment of non-polar MoS_2 systems remain almost unchanged, and the polar MoSSe vary linearly with extra electric field E_{ext} . And it needed the external negative electric field of $E_{\text{ext}} = -0.14 \text{ V/\AA}$ to accommodate the intrinsic dipole moment.

3. The compare Rashba splitting for monolayer MoSe₂ and MoS₂

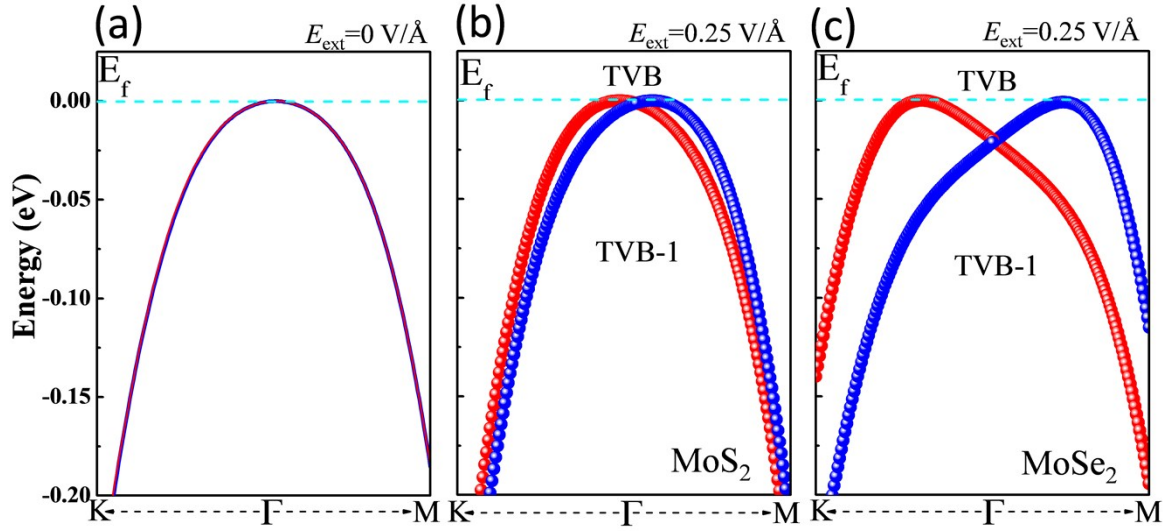


Figure S3 (a) The enlarged view of TVB of band structure for monolayer MoSe₂ or MoS₂ around the Γ point without the external electric field. (Spin up and down are degeneration) (b), (c) The enlarged view of TVB of band structure for monolayer MoSe₂ or MoS₂ around the Γ point with the electric field $E_{\text{ext}} = 0.25 \text{ V/\AA}$. The dot size along the Γ -K and Γ -M direction denotes the expected value of spin operator $\langle S_{\alpha}(\vec{k}) \rangle$ ($\alpha = x, y$). The red and blue color represents the spin up and down band, respectively. The VBM is set to zero.

Figure S3a show the Rashba splitting for monolayer MoSe₂ or MoS₂ at Γ point without the external field. The topmost valence bands are set to zero. (The red and blue) represent the spin up and spin down). The spin up and spin down are degeneration. From Figure S3b-c we can clear see that the external electric field $E_{\text{ext}} = 0.25 \text{ V/\AA}$ (it is easy to be reach by the experimental level in ionic liquid gate) can induce a larger isotropic spin splitting in MoSe₂. (See details in main text)

4. The Rashba splitting and spin texture for MoSe₂

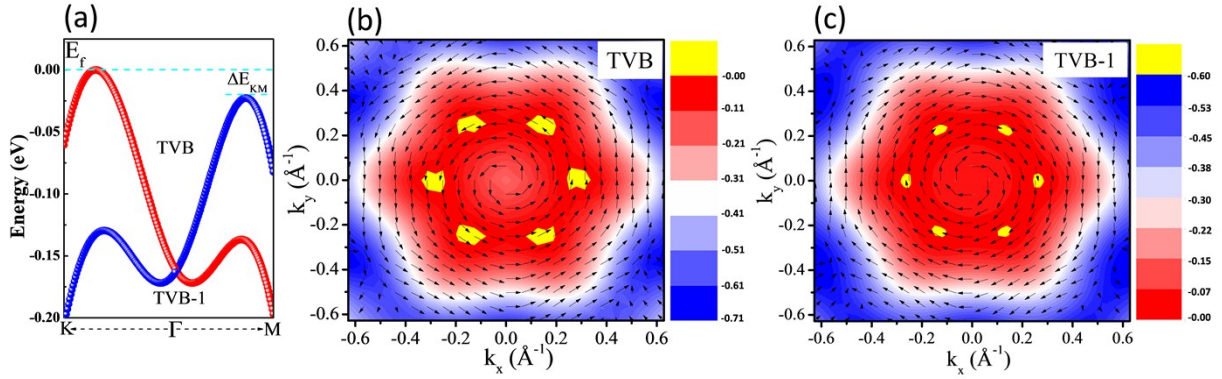


Figure S4 (a) The enlarged view of TVB of band structure for MoSe₂ around the Γ point with the increase field $E_{\text{ext}} = 0.70 \text{ V/\AA}$. The dot size along the Γ -K and Γ -M direction denotes the expected value of spin operator $\langle S_{\alpha}(\vec{k}) \rangle$ ($\alpha = x, y$). The red and blue color represents the spin up and down band, respectively. The VBM is set to zero. (b), (c) The energy contour and spin texture of the top valence band TVB and the neighboring band below TVB-1 around the Γ point with electric field $E_{\text{ext}} = 0.70 \text{ V/\AA}$.

Figure 4a show the Rashba splitting for MoSe₂ at Γ point with the external field $E_{\text{ext}} = 0.70 \text{ V/\AA}$. The topmost valence bands are set to zero. (The red and blue) represent the spin up and spin down). Figure S4 b and c show the energy contour and spin texture of the top valence band (TVB) and its neighboring band (TVB-1) around the Γ point. (See details in main text)

5. The Rashba splitting of MoSSe

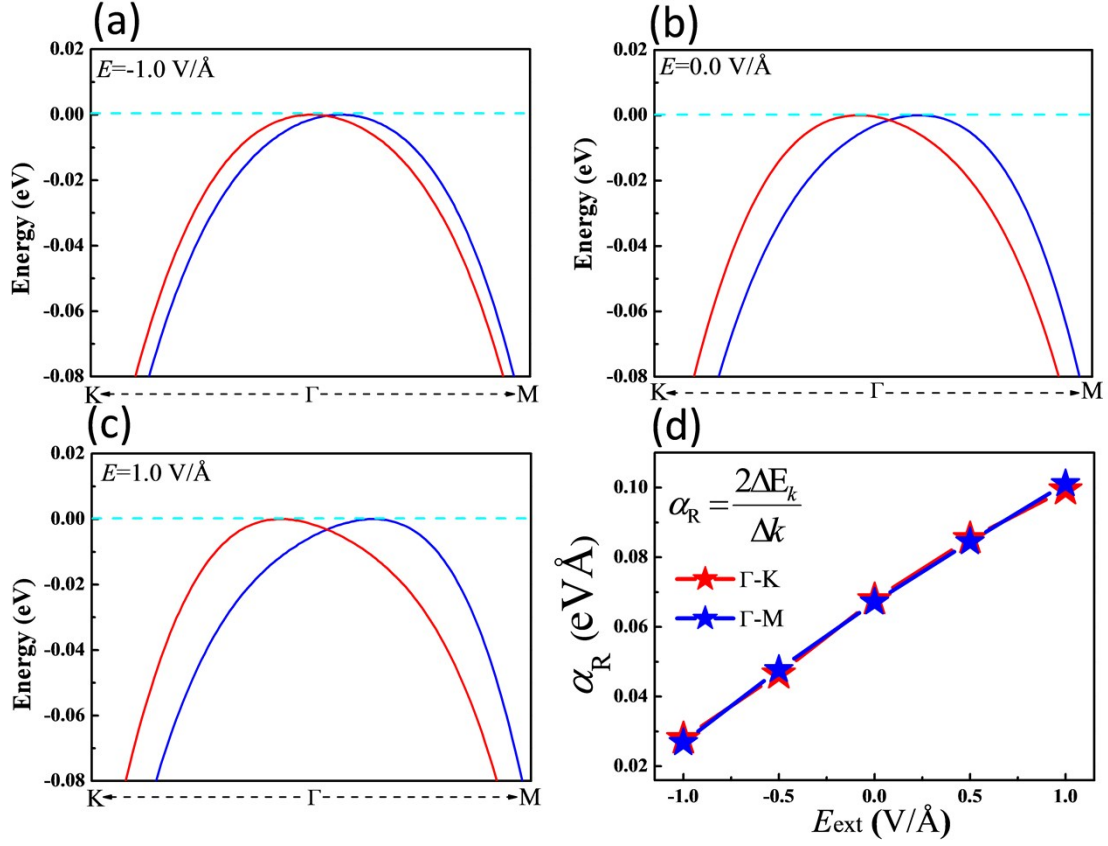


Figure S5 (a)-(c) The Rashba splittings for MoSSe with field $E_{\text{ext}} = -1.0 \text{ V/Å}$, $E_{\text{ext}} = 0.0 \text{ V/Å}$, and $E_{\text{ext}} = 1.0 \text{ V/Å}$. The topmost valence bands are set to zero. The spin up and spin down electrons are represented by the red and blue lines. (d) The Rashba splitting is linear with the extra electric field with formula $\alpha_R = \frac{2\Delta E}{\Delta k}$. Blue star and red star represent α_R along the Γ M and Γ K directions, respectively.

Figure S5a-c show the Rashba splitting for MoSSe with field $E_{\text{ext}} = -1.0 \text{ V/Å}$, 0.0 V/Å , and 1.0 V/Å . The topmost valence bands are set to zero. (The red and blue) represent the spin up and spin down). From Figure S5 we can see that α_R^{iso} of MoSSe has linear dependence on the electric field. Negative (positive) electric field increases (decreases) the α_R^{iso} of MoSSe.

6. The nonlinear Rashba splitting of MoSe₂

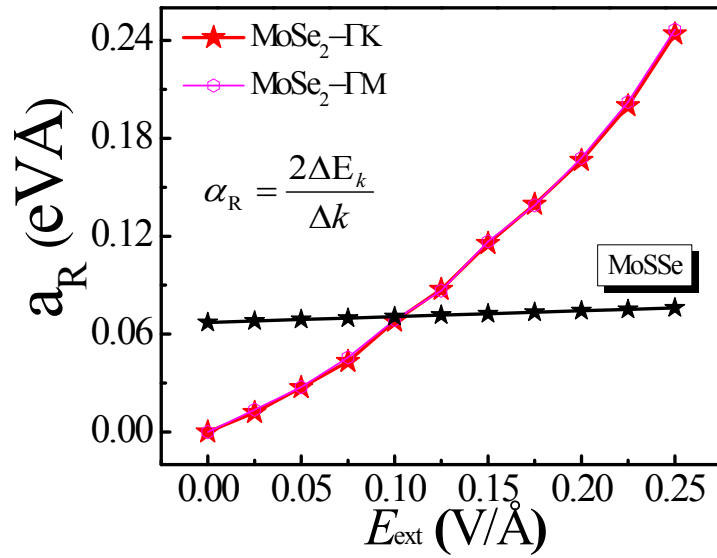


Figure S6 The linear Rashba parameters calculated by $\alpha_R = \frac{2\Delta E}{\Delta k}$ along Γ -K (filled symbols) and Γ -M (empty symbols) direction. For comparison, the data for MoSSe are also shown (black stars).

Figure S6 shows the zoom in plot as that in Fig. 4a. It is clearly seen that Rashba spin splitting of MoSe₂ deviates from the linear behavior in the experimentally accessible conditions ($E_{\text{ext}} = 0.27 \text{ V/\AA}$).

7. The Rashba splitting of MoSe₂ and WSe₂

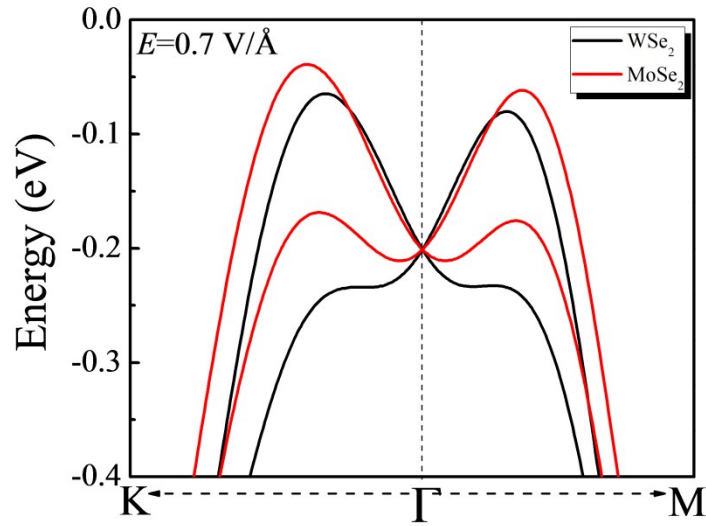


Figure S7 The enlarged view of TVB of band structure for MoSe₂ and WSe₂ under the field $E_{\text{ext}} = 0.70 \text{ V/\AA}$

Figure S7 show the Rashba splitting for MoSe₂ (red) and WSe₂ (black) with field $E_{\text{ext}} = 0.70 \text{ V/\AA}$. From Figure S5 we clearly see that the anisotropic energy splitting $\Delta_{\text{K-M}}$ of MoSe₂ (22.7 meV) is slightly larger than WSe₂ (15.7 meV).

References:

1. Z. Y. Zhu, Y. C. Cheng and U. Schwingenschlögl, *Phys. Rev. B* 2011, **84**, 153402.
2. Y. C. Cheng, Z. Y. Zhu, M. Tahir and U. Schwingenschlögl, *EPL* (Europhysics Letters) 2013, **102**, 57001.
3. H. L. Zhuang and R. G. Hennig, *J. Phys. Chem. C* 2013, **117**, 20440-20445.
4. A. Splendiani, L. Sun, Y. Zhang, T. Li, J. Kim, C. Y. Chim, G. Galli and F. Wang, *Nano Lett.* 2010, **10**, 1271-1275.
5. S. Tongay, J. Zhou, C. Ataca, K. Lo, T. S. Matthews, J. Li, J. C. Grossman and J. Wu, *Nano Lett.* 2012, **12**, 5576-5580.
6. Y. Zhang, T. R. Chang, B. Zhou, Y. T. Cui, H. Yan, Z. Liu, F. Schmitt, J. Lee, R. Moore, Y. Chen, H. Lin, H. T. Jeng, S. K. Mo, Z. Hussain, A. Bansil and Z. X. Shen, *Nat. Nanotechnol.* 2014, **9**, 111-115.